Research Paper

Mitochondrial permeability transition pore contributes to mitochondrial dysfunction in fibroblasts of patients with sporadic Alzheimer's disease

María José Pérez[a,b], Daniela P. Ponce[c,d], Alejandra Aranguiz[a,b], Maria I. Behrens[c,d], Rodrigo A. Quintanilla[a,b,*]

[a] Laboratory of Neurodegenerative Diseases, Universidad Autónoma de Chile, Santiago, Chile
[b] Centro de Investigación y Estudio del Consumo de Alcohol en Adolescentes (CIAA), Santiago, Chile
[c] Instituto de Ciencias Biomédicas, Universidad de Chile, Chile
[d] Centro de Investigación Clínica Avanzada (CICA), Hospital Clínico Universidad de Chile, Chile

ABSTRACT

In the last few decades, many reports have suggested that mitochondrial function impairment is a hallmark of Alzheimer's disease (AD). Although AD is a neurodegenerative disorder, mitochondrial damage is also present in patients' peripheral tissues, suggesting a target to develop new biomarkers. Our previous findings indicate that AD fibroblasts show specific defects in mitochondrial dynamics and bioenergetics, which affects the generation of adenosine triphosphate (ATP). Therefore, we explored the possible mechanisms involved in this mitochondrial failure. We found that compared with normal fibroblasts, AD fibroblasts had mitochondrial calcium dysregulation. Further, AD fibroblasts showed a persistent activation of the non-specific mitochondrial calcium channel, the mitochondrial permeability transition pore (mPTP). Moreover, the pharmacological blockage of mPTP with Cyclosporine A (CsA) prevented the increase of mitochondrial superoxide levels, and significantly improved mitochondrial and cytosolic calcium dysregulation in AD fibroblasts. Finally, despite the failure of CsA to improve ATP levels, the inhibition of mitochondrial calcium uptake by the mitochondrial calcium uniporter increased ATP production in AD fibroblasts, indicating that these two mechanisms may contribute to mitochondrial failure in AD fibroblasts. These findings suggest that peripheral cells present similar signs of mitochondrial dysfunction observed in the brain of AD patients. Therefore, our work creates possibilities of new targets to study for early diagnosis of the AD.

1. Introduction

AD is typically a late-onset disorder and represents the most common form of dementia among the aging population [17]. AD is characterized by the presence of different aggregates of misfolded proteins in the brain, namely amyloid beta peptides (Aß) and neurofibrillary tangles (NFTs); these tangles are generated by pathological forms of the tau protein [30]. Another important hallmark of AD is mitochondrial dysfunction, which regularly appears prior to tau and Aß pathology [30]; this mitochondrial dysfunction contributes to the synaptic and neuronal damage observed in AD [37,5].

One of the principal functions of the mitochondria is to convert energy derived from nutrients into adenosine triphosphate (ATP) [23]. Current evidence suggests that in AD brains, mitochondrial dysfunction is commonly presented as a reduction in ATP synthesis, increase in reactive oxygen species (ROS) production, impairment of calcium homeostasis, and an imbalance in mitochondrial dynamics [22,5]. More importantly, mitochondrial damage is not only an early and progressive feature present in the AD brain, but also has been found in peripheral tissues derived from AD patients [27,34,37,7]. Our prior research suggests that fibroblasts obtained from AD patients demonstrate a significant alteration in mitochondrial length and dynamics [27]. Additionally, AD fibroblasts show an impaired mitochondrial bioenergetics profile compared to aged-matched and young patients' cells [27].

Despite our findings suggesting that peripheral fibroblasts could replicate the mitochondrial failure observed in the AD brain, the underlying mechanisms are currently unknown.

Recent studies have suggested that the mitochondrial permeability transition pore (mPTP) could be playing a role in the metabolic stress observed in AD [10,16,28]. The genetic removal of the Cyclophilin D (CypD) protein, a key component of the mPTP, prevents against mitochondrial dysfunction and improves synaptic and cognitive loss. This is seen in transgenic AD models that demonstrate the overexpression of an amyloid precursor protein (APP) [10,9]. Furthermore, cultured neurons obtained from CypD knock-out mice showed a decrease in Aβ-dependent ROS generation, increase in the calcium buffering capacity, improved mitochondrial respiratory function, and attenuation of abnormalities in synaptic plasticity present in AD [10,16]. These findings suggest opening of the mPTP could be responsible for the mitochondrial dysfunction observed in the AD brain; however, its contribution to mitochondrial failure in AD peripheral cells remains elusive. Therefore, we studied the contribution of the mPTP and calcium dysregulation in mitochondrial impairment present in fibroblasts obtained from AD and aged-matched patients.

2. Methods

2.1. Patients and cell culture fibroblasts

Skin fibroblasts were obtained from six AD-patients and five age-matched healthy controls, and they were cultured in growth media containing MEMα (Biological Industries), with 10% FBS (Gibco) and 1% penicillin-streptomycin (Corning) [35]. To prevent mPTP opening, cells were pre-treated with 0.5 μM Cyclosporine A (CsA; Tocris, Bioscience) for 2 h, as recommended by the manufacturer. To study mitochondrial calcium uniporter (MCU) participation, cells were treated with 20 μM Ruthenium Red (RRed; Tocris, Bioscience) for 1 h, as indicated. All patients were recruited after providing informed consent, and the study was approved by the Ethics Committee of the Hospital Clínico de la Universidad de Chile and Universidad Autónoma de Chile. AD diagnosis was established according to tests by the National Institute of Neurological and Communicative Diseases and Stroke-AD and Related Disorders Association [24], as well as the Clinical Dementia Rating (CDR) scale, as shown in Table 1 [25]. For the age of the patients, fibroblasts donors are not believed to carry any autosomal dominant mutations as the main cause of AD. The APOE genotype presence in AD and age-match non-demented fibroblasts is unknown.

This table represents the number of patients, age range, sex, Montreal Cognitive Assessment (MoCA) test scores, and diagnosis type for each patient according to the cognitive tests applied. The maximum score for the MoCA is 30, with lower scores associated with greater cognitive deterioration.

2.2. Determination of mitochondrial superoxide and ROS levels

ROS levels were evaluated using chloromethyl-2,7-dichlorodihydrofluorescein diacetate (DCF) dye (Molecular Probes, OR, USA); mitochondrial superoxide levels were determined using MitoSOX Red (Molecular Probes, OR, USA) in conjunction with the mitochondrial marker Mitotracker Green (MGreen; Molecular Probes, OR, USA).

Cultured fibroblasts were incubated with 10 μM DCF, 0.5 μM MitoSOX, or 100 nM MGreen in Krebs-Ringer-HEPES (KRH)-glucose buffer at 37 °C for 30 min [32]. Images were taken by adjusting to the same exposure time and gain detector to diminish the photo-bleaching effect of the dye [32]. Quantification of fluorescence intensity for each separate experiment was carried out by analyzing the signal intensity of 25 images for every indicated condition, using Image J software. Results from the three independent experiments were expressed as the average fluorescence intensity, per area, in every image. Fluorescence images were taken with a high-resolution fluorescence microscopy (Leica LX6000, Germany) using a 63x oil objective.

2.3. Mitochondrial and cytosolic calcium measurements

Cytosolic calcium levels were evaluated using Fluo-3AM dye (Molecular Probes, OR, USA), and mitochondrial calcium levels were determined using Rhod-2AM (Molecular Probes, OR, USA) in conjunction with MGreen. Fibroblasts were loaded with 1 μM Fluo-3 AM, or 0.5 μM Rhod-2AM with 0.1 μM MGreen in KRH-glucose buffer at 37 °C for 30 min [32]. For basal mitochondrial calcium measurements, Rhod-2 fluorescence intensity was determined from at least 25 images for every indicated condition, using Image J software. Results from the three independent experiments were expressed as the average fluorescence intensity, per area, in every image. To determine changes in calcium levels in basal conditions, we analyzed the fluorescence intensity (Fluo-3 or Rhod-2) of 5 images in each experiment for every independent condition. To determinate dynamic calcium changes, we treated the cells with thapsigargin (10 μM) for 20 min and we measure fluorescence intensity (Fluo-3 or Rhod-2) from at least 15 cells on average, per experiment. Fluorescent background was subtracted from the dye fluorescence measurements in every experiment, as previously described [32]. Fluorescence intensity and quantification of the three independent experiments were made using Image J software (NIH).

2.4. Determination of ATP levels

Total ATP levels were measured in fibroblasts whole lysate using a luciferin/luciferase bioluminescence assay kit (ATP Determination Kit #A22066, Molecular Probes, Invitrogen). The amount of ATP in each sample was calculated from standard curves and normalized to the total protein concentration.

2.5. Reverse transcription and real-time PCR

RNA was isolated from cells using TRIZOL (Invitrogen, Life Technologies) and eluted in RNase free water, according to the manufacturer's protocol. Extracted RNA was treated with RNase free-DNase I, Amplification Grade, (Invitrogen) to remove traces of contaminating DNA and it was then heat-treated to inactivate DNase I and precipitated with ethanol to clean up the reaction. One microgram of RNA was subjected to reverse transcription using ImProm-II Reverse Transcription System (Promega), following the manufacturer's protocol.

A real-time polymerase chain reaction (PCR) was performed in triplicate in the LightCycler® 96 System (Roche Diagnostics GmbH, Roche Applied Science, Mannheim, Germany) using KAPA SYBR FAST qPCR Master Mix (2 ×). Amplification conditions consisted of an initial hot start at 95 °C for 10 min, followed by amplification of 40 cycles (95 °C

Table 1
Demographic characteristics of the patients.

Abbreviations	Number of patients	Range Age	Percent women	MoCA Test range	Diagnostic
NP	5	70–85	100	25–30	Control
MCI	2	75–85	100	13–19	Mild cognitive decline AD
ADP	4	65–80	50	0–6	Severe cognitive decline AD

Table 2
List of primers for real-time PCR studies.

Gene	Primer	Sequence
Complex V (ATP5F1)	Forward primer	5′- ACTGGGCAACAGTGGATCTC-3′
	Reverse primer	5′- CTTGGTGCCAATTGGTCGTG -3′
ANT	Forward primer	5′- CACCCATCGAGAGGGTCAA -3′
	Reverse primer	5′- ATTTGCTTGCTGGCATGCT -3′
VDAC	Forward primer	5′- GCCCTACCTGATTGGTGCAA -3′
	Reverse primer	5′- TTCAAGCTCCCTGGCAGAA -3′
CypD	Forward primer	5′- AGCCCTCCAACCCCAGTAA -3′
	Reverse primer	5′- CGCTCCCCTCCGATGTC -3′
GAPDH	Forward primer	5′- GAGTCAACGGATTTGGTCGT-3′
	Reverse primer	5′- TTGATTTTGGAGGGATCTCG -3′

for 15 s, 60 °C for 20 s, and 72 °C for 20 s). Melting curve analysis was performed immediately after amplification from 55° to 95°C, and values were normalized to glyceraldehyde 3-phosphate dehydrogenase (GAPDH) expression levels using the ΔCT method. Lists of primers used in real-time PCR are described in Table 2.

The table summarizes the forward and reverse primers used for real-time PCR.

2.6. Western blot analysis

Cells were lysed in Triton lysis buffer, which included a protease inhibitor cocktail (Roche) and a phosphatase inhibitor [27,29]. Thirty micrograms of total protein extracts were resolved on a 10% SDS-electrophoresis gel and transferred to nitrocellulose membranes. After the blocking process, membranes were incubated with mouse mono-clonal anti-CypD (Santa Cruz, 1:1000 dilution), anti-voltage dependent anion channel (VDAC; Santa Cruz, 1:1000 dilution), anti-adenine nu-cleotide translocator (ANT; Santa Cruz, 1:1000 dilution), anti-oligo-mycin sensitivity conferring protein (OSCP; Santa Cruz, 1:1000 dilu-tion), anti-MCU sensitivity conferring protein (OSCP; Santa Cruz, 1:1000 dilution) antibodies. The equal loading and transfer of mem-branes was subsequently retested with anti-tubulin antibody (Thermo Fisher, 1:2000). Protein signal was revealed using an HRP-linked goat anti-mouse or anti-rabbit secondary antibody (Thermo Fisher, 1:2000), as suggested by the manufacturer. Finally, the immunoreactive protein signal was detected using an enhanced chemiluminescence reaction (Thermo Fisher).

2.7. In situ evaluation of the mPTP opening

The opening of the mPTP was determinate in cells previously treated with 50 mM cobalt chloride for 15 min, before incubation with 1 μM Calcein Green AM (Molecular Probes, OR, USA) and 0.5 μM Mitotracker Red (Molecular Probes, OR, USA) in KRH-glucose buffer at 37 °C for 30 min [32]. Quenching of free Calcein by cobalt chloride allowed the preservation of mitochondrial integrity as an mPTP in-dicator [18,31]. Quantification of fluorescence intensity for three se-parate experiments was carried out by analyzing the Calcein intensity in 25 images for every indicated condition using Image J software.

2.8. Mitochondrial membrane potential determinations

The mitochondrial potential was determined using the mitochon-drial dye tetramethyl-rhodamine methyl ester (TMRM) in non-quenching mode, as described previously with modifications [32,36]. Mitochondrial potential levels were expressed as the average of fluor-escence signal (F) per area in every image, and then subtracted by the intensity of background fluorescence (F0). Fibroblasts were preloaded with TMRM (100 nM) in KRH-glucose buffer at 37 °C for 45 min, and cells were then treated with 10 μM thapsigargin for 30 min. For the three independent experiments, the intensity of the signal was analyzed

in 30 cells, measuring 25 images per experiment in each patient using Image J software.

2.9. Immunofluorescence

Fibroblasts were fixed in 4% paraformaldehyde-KRH for 15 min at 37 °C. After blocking (5% bovine serum, 0.1% triton X-100, KRH for 1 h), cells were incubated with antibodies against MCU (Santa Cruz, 1:200). After washing in PBS, the cells were probed with a secondary antibody, Alexa Fluor 488 (Life Technologies, 1:1000), and DAPI (Sigma, 1:5000) staining was performed. For the three independent experiments, we analyzed fluorescence intensity from 30 to 40 cells, measuring 25 images for each patient, using Image J software.

2.10. Statistical analysis

We used a Student's t-test to analyze statistical differences between the two groups of data. Differences were considered significant if p < 0.05 or p < 0.001, as indicated.

3. Results

3.1. Mitochondrial bioenergetics is altered in fibroblasts from AD patients

In our previous work, we observed that AD fibroblasts demonstrated a basal increase in ROS levels, and a cytosolic calcium dysregulation in response to calcium overload stimuli using thapsigargin [27]. To extend these findings, we evaluated mitochondrial superoxide levels in healthy and AD fibroblasts using the specific Mitosox dye (Fig. 1A, B). Fig. 1A shows a representative set of fluorescence images of Mitosox staining in control and AD fibroblasts. Analysis of fluorescence images showed a significant increase in Mitosox fluorescence levels in AD fibroblasts than in healthy cells (Fig. 1A, B, Supplementary Fig. 1A). To complete these observations, we analyzed the mitochondrial calcium levels in AD fibroblasts using Rhod-2AM dye (Fig. 1C, Supplementary Fig. 1B). Analysis of the fluorescence intensity indicated a significant decrease in mitochondrial calcium levels in AD fibroblasts than in control patients' cells (Fig. 1D). Further, we studied the changes in mitochondrial cal-cium levels in response to calcium overload stimuli induced by thap-sigargin [27]. We measured the relative intensity levels of Rhod-2AM after thapsigargin treatment for 25 min (Fig. 1E). We observed that after an initial increase of mitochondrial calcium, AD fibroblasts showed a time-dependent decrease of mitochondrial calcium levels compared to that of control fibroblasts (Fig. 1E). Previously, we ana-lyzed total ATP levels in whole fibroblast extracts from AD and control patients [27]. In these studies, we only detected significant differences in two of the three AD patients analyzed [27]. In that context, other groups had found that mitochondrial damage progress, as well as cognitive decline in the brains of AD patients [22]. Hence, we de-termined ATP levels, increased the number of patients, and analyzed the results in accordance to their respective cognitive decline progress score. Disease patients were separated into two groups: mild cognitive impairment (MCI) and severe cognitive impairment AD (Fig. 1F). Therefore, we found a significant decrease in ATP levels in severe AD patients that differentiated them from control and MCI patients (Fig. 1F).

3.2. Fibroblasts of AD patients present an open state of the mPTP

To evaluate if the mPTP channel is actively participating in mi-tochondrial failure observed in AD fibroblasts, we first studied the protein expression levels of major mPTP components: cyclophilin D (CypD), ANT, VDAC, and ATP synthase [28]. We found that AD patients demonstrated a significant decrease in protein expression of CypD, VDAC, OSCP, and the ATP synthase subunit; these have been described to be involved in mPTP formation (Fig. 2A, B) [28]. In complementary
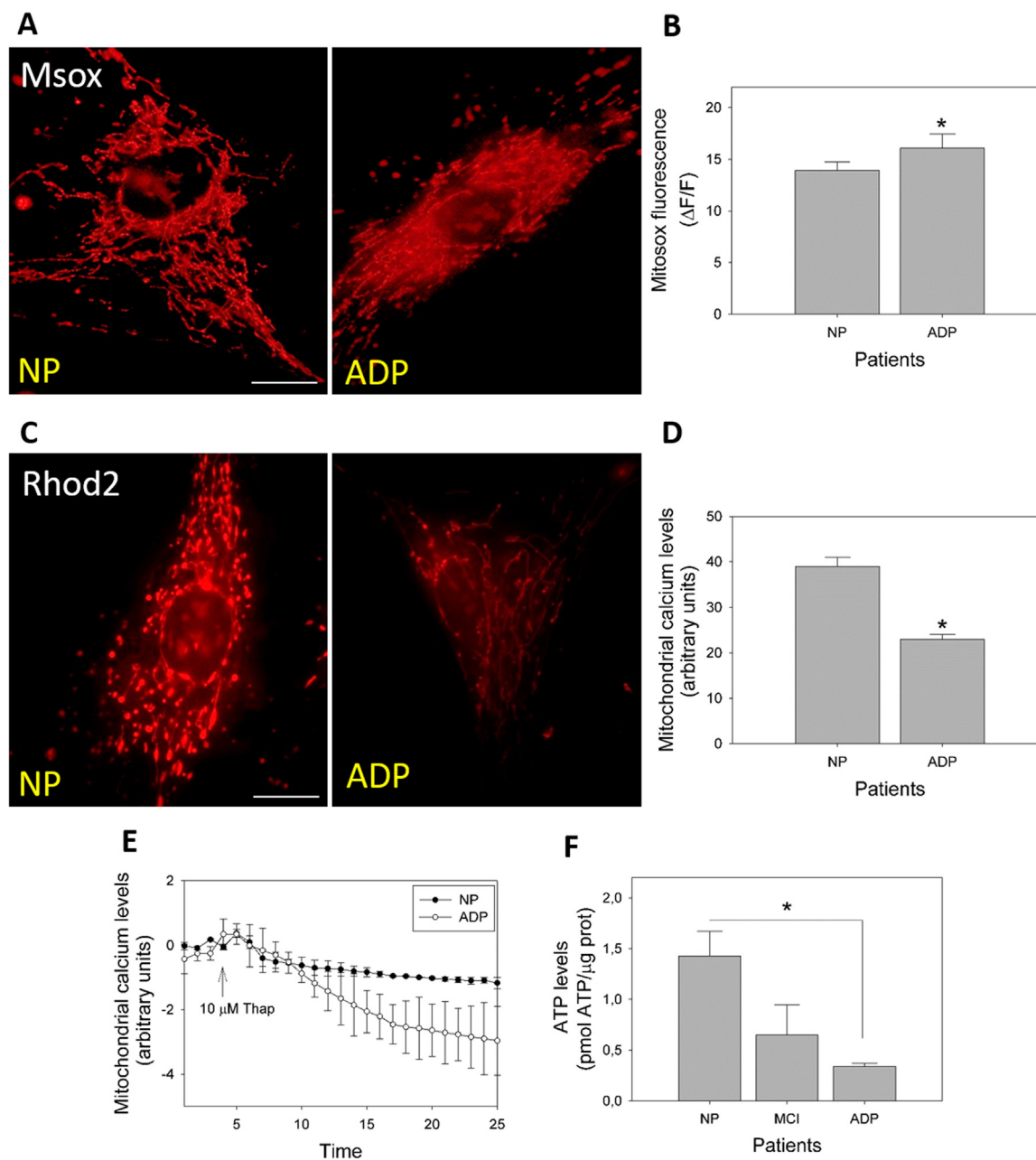
Fig. 1. Analysis of mitochondrial calcium regulation and superoxide production in fibroblasts from AD patients. A. Cells were loaded with MitoSOX to determine mitochondrial superoxide production. Bar = 10 μm **B.** Quantification of the MitoSox mitochondrial intensity signal. Data represented as are mean ± standard error (SE); n = 3 technical replicates for each subject. *$p < 0.05$ indicates differences between groups calculated by Student's *t*-test. **C.** Cells were loaded with Rhod-2 AM to determine mitochondrial calcium levels. Bar = 10 μm **D.** Quantification of relative mitochondrial calcium levels as arbitrary units. Data are represented as mean ± SE; n = 3 technical replicates for each subject. *$p < 0.05$ indicates differences between groups calculated by Student's *t*-test. **E.** Representative trends of mitochondrial calcium levels over 25 min in AD and control fibroblasts. After 5 min, cells were treated with thapsigargin (arrow). Data are represented as mean ± SE; n = 3 technical replicates for each subject. **F.** Total ATP levels from control, MCI, and severe cognitive impairment AD fibroblasts. Data are represented as mean ± SE; n = 3 technical replicates for each subject. *$p < 0.05$ indicates differences with controls calculated by Student's *t*-test.

studies, we analyzed mRNA levels in the same mPTP components, which showed a significant increase in CypD, ANT, and OSCP in AD fibroblasts than that in healthy fibroblasts (Fig. 2C). *In situ*, we determined the formation and subsequent opening of the mPTP by measuring the retention of Calcein AM fluorescent intensity inside the mitochondria, in conjunction with Mitotracker Red staining (Fig. 3). We found that normal fibroblasts showed a significant mitochondrial localization pattern of Calcein AM (Fig. 3A, B; Supplementary Fig. 2A), which suggests a closed state of the mPTP [32]. Alternatively, MCI fibroblasts showed a partial decrease in mitochondrial/Calcein AM localization signal (Fig. 3A, B; Supplementary Fig. 2A); more interesting

is that severe AD fibroblasts showed a complete reduction in mitochondrial/Calcein AM fluorescence intensity (Fig. 3A, B; Supplementary Fig. 2A). These findings suggest an mPTP transient opening for MCI cells and a full, permanent, open state for AD cells [18,32].

3.3. Cyclosporin A treatment inhibited mPTP opening in AD cultured fibroblasts

To evaluate the pharmacological closure of the mPTP, we treated AD and control fibroblasts with CsA [31], a fungus-derived drug that
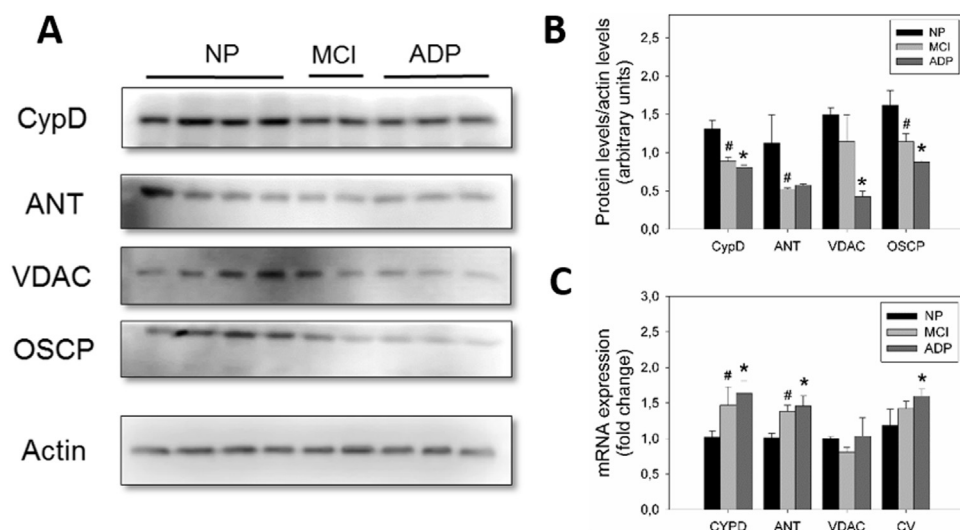
Fig. 2. Expression of the principal protein components of the mPTP in AD fibroblasts. A. Representative images of protein levels of mPTP components CypD, VDAC, ANT, and OSCP, in AD, MCI, and control patients determined by western blot (see Methods). **B.** Quantitative analysis of relative protein expression. Data are represented as mean ± SE. **C.** Normalized levels of mRNA content from mPTP components CypD, VDAC, ANT, and OSCP. #$p < 0.05$ indicates differences between control and MCI. *$p < 0.05$ indicates differences between control and AD patients calculated by Student's *t*-test; data are represented as mean ± SEM.

reduces the mPTP opening through its specific binding with CypD [15,32]. Here, we observed that AD fibroblasts treated with CsA showed a significant increase in the mitochondrial/Calcein AM localization than that in untreated AD fibroblasts, which suggests the closure of mPTP (Fig. 3C; Supplementary Fig. 2B).

3.4. mPTP blockage reduced oxidative stress and mitochondrial superoxide levels in AD fibroblasts

To evaluate the contribution of the mPTP opening in the oxidative stress observed in AD fibroblasts, we analyzed DCF and MitoSox fluorescence levels in AD and control cells treated with CsA (Fig. 4). Fig. 4A shows representative fluorescence images of DCF in control, MCI, and severe AD cells in the absence or presence of CsA (Fig. 4A). MCI and AD fibroblasts showed a significant increase in ROS levels, and CsA treatment significantly reduced DCF fluorescence signal intensity (Fig. 4C). Additionally, CsA treatment significantly reduced mitochondrial superoxide levels in MCI and severe AD patients (Fig. 3B, D).

3.5. Cyclosporin A treatment prevent calcium dysregulation present in AD fibroblasts

To evaluate the contribution of mPTP to the calcium dysregulation observed in AD fibroblasts, we analyzed cytosolic (Fluo-3 AM) and mitochondrial (Rhod-2 AM) calcium levels before and after CsA treatment (Fig. 5). We first evaluated the relative levels of cytosolic calcium after the pre-treatment with 5 µM of CsA in response to 10 µM thapsigargin (Fig. 5A). Calcium overload with thapsigargin induced a significant cytosolic calcium peak in controls patients' cells (Fig. 5A, B); however, a significantly higher increase in cytosolic calcium levels was observed in MCI and severe AD fibroblasts than in control patients (Fig. 5B). Moreover, CsA treatment inhibited this cytosolic calcium increase in MCI and AD fibroblasts, in which levels were equal to control cells after thapsigargin stimulation (Fig. 5B). mPTP inhibition with CsA significantly decreased mitochondrial calcium release in MCI and severe AD fibroblasts exposed to thapsigargin (Fig. 5C, D). In our previous work, we described that in basal conditions, there are no changes in mitochondrial potential levels (MMP) between controls and AD patients; however, after a calcium stress stimuli using thapsigargin, AD fibroblasts showed a significant mitochondrial depolarization compared to healthy cells [27]. Furthermore, we studied the changes in MMP in response to thapsigargin treatment (Fig. 5E). We observed that AD fibroblasts presented a significant decrease in MMP (Fig. 5E, F), and the CsA treatment partially restored mitochondrial potential levels in AD fibroblasts (Fig. 5E, F). Interestingly, there were no changes in ATP

levels of MCI, nor severe AD patients' fibroblasts after CsA treatment (Fig. 5G).

3.6. Inhibition of mitochondrial calcium uptake prevented mitochondrial bioenergetics defects in AD fibroblasts

Exaggerated accumulation of calcium in mitochondria can lead to overload and impairment of mitochondrial function, due to the opening of the mPTP [8]. However, we observed that CsA treatment only partially restores the decreased mitochondrial calcium and MMP levels in AD fibroblasts, suggesting a possible role of MCU in mitochondrial failure in AD fibroblasts. Therefore, we evaluated the expression of one of the primary sources of mitochondria calcium uptake [8], the MCU (Fig. 6A). Interestingly, we observed that fibroblasts of AD patients showed a significant increase in MCU content than that in the control patients (Fig. 6A-D). Moreover, the pharmacological inhibition of MCU activity with RRed [4] completely restored mitochondrial calcium and mitochondrial potential levels after thapsigargin treatment (Fig. 5E–G, Supplementary Fig. 3A). Additionally, the inhibition of mitochondrial calcium uptake with RRed increased ATP levels in MCI and severe AD patients (Fig. 5H, Supplementary Fig. 3B). These important findings suggest that mitochondrial calcium uptake could be contributing to the mitochondrial impairment induced by the mPTP in AD fibroblasts.

4. Discussion

Mitochondrial dysfunction is an important component of the pathogenesis of AD [5], as defects in mitochondria have been consequently observed in several AD mouse and neuronal cell models [5]. Peripheral AD cells show different degenerative signs than those present in AD neurons, including oxidative stress, calcium deregulation, and mitochondrial injury [27,34,37,7]. In our previous work, we showed that AD fibroblasts presented a significant reduction in mitochondrial length with important changes in the expression of proteins that control mitochondrial fusion [27]. Moreover, AD fibroblasts showed a specific alteration in the proteolytic processing of OPA1, a master regulator of mitochondrial fusion [27]. On the other hand, we and others also established that fibroblasts from AD patients present higher levels of ROS than those of age-matched controls [14,26,27,7], here we show that AD fibroblasts present an increase in superoxide production by mitochondria compared to control cells. However, previous evidence suggests that fibroblasts from AD patients show impairment in calcium homeostasis that could later negatively impact mitochondrial health [19,27,33]. Here, we demonstrated that fibroblasts of AD patients present lower basal mitochondrial calcium levels
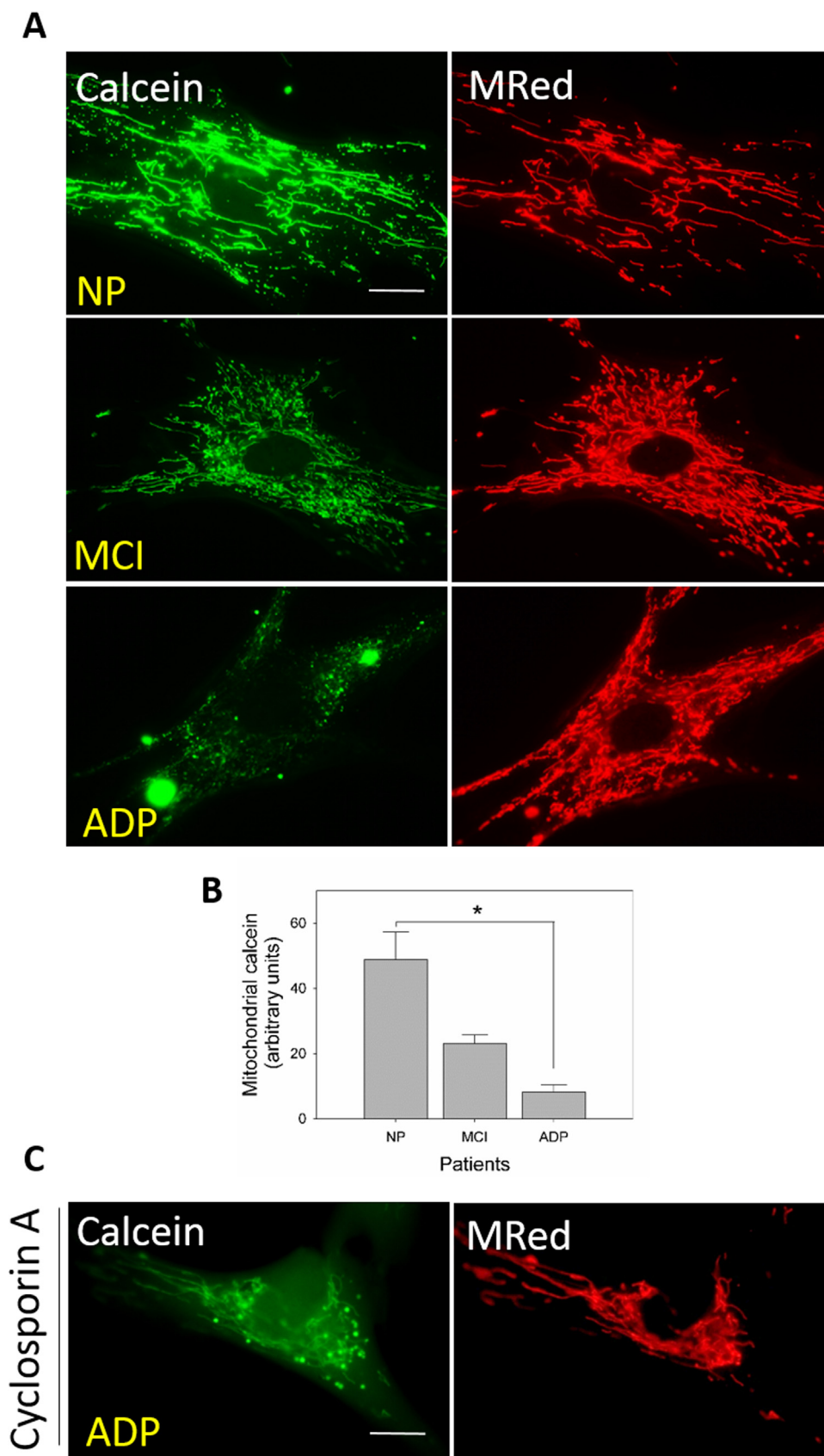
Fig. 3. AD fibroblasts present an active mPTP opened state. A. Cells were loaded with cobalt chloride, Calcein AM (Green) to determine the opening of the mPTP, and Mitotracker Red to determine mitochondrial morphology. Bar = 10 μm **B**. Quantification of the Calcein mitochondrial signal from control, MCI, and severe cognitive impairment AD fibroblasts. Data are represented as mean ± SE; n = 3 technical replicates for each subject. *p < 0.05 indicates differences between groups calculated by Student's *t*-test. **C.** AD fibroblasts were loaded with cobalt chloride and Calcein Green to determinate opening of the mPTP after CsA treatment. Bar = 10 μm.
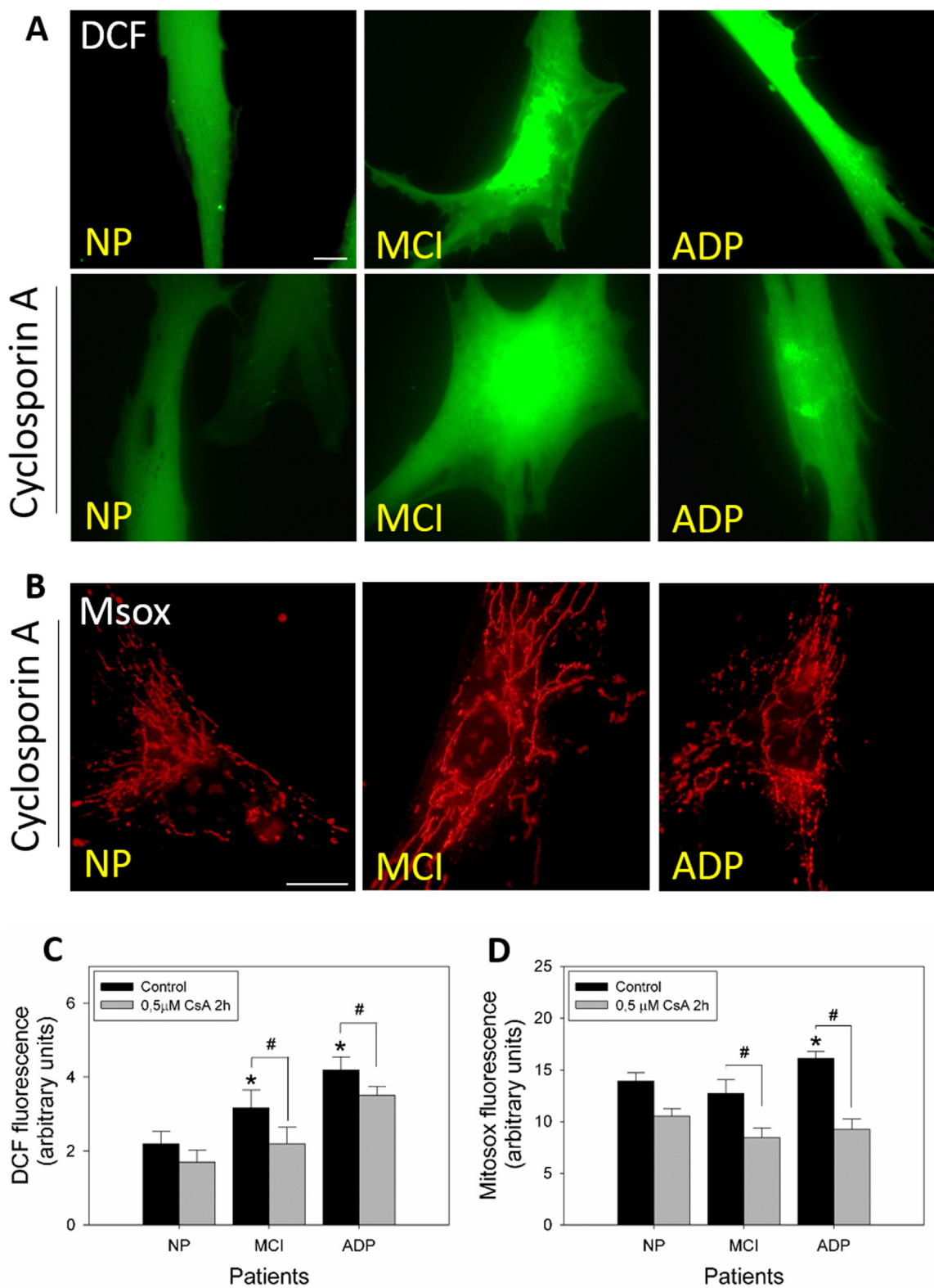
Fig. 4. Inhibition of mPTP opening prevents oxidative stress and mitochondrial superoxide levels in fibroblasts of AD patients. A. Representative fluorescent images of DCF intensity before and after treatment with CsA. Bar = 10 µm **B**. Representative fluorescent images of MitoSOX intensity after treatment with CsA. Bar = 10 µm **C**. Graph showing quantitative data of ROS levels for all fibroblasts. Data are represented as mean ± SE; n = 3 technical replicates for each subject. *p < 0.05 indicates differences with control patients, #p < 0.05 indicates differences between control and CsA treatment calculated by Student's *t*-test. **D**. Graph showing quantitative data of superoxide levels in each patient's cell type. Data are represented as mean ± SE; n = 3 technical replicates for each subject. *p < 0.05 indicates differences between AD and control patients, #p < 0.05 indicates differences between control and CsA treatment calculated by Student's *t*-test.
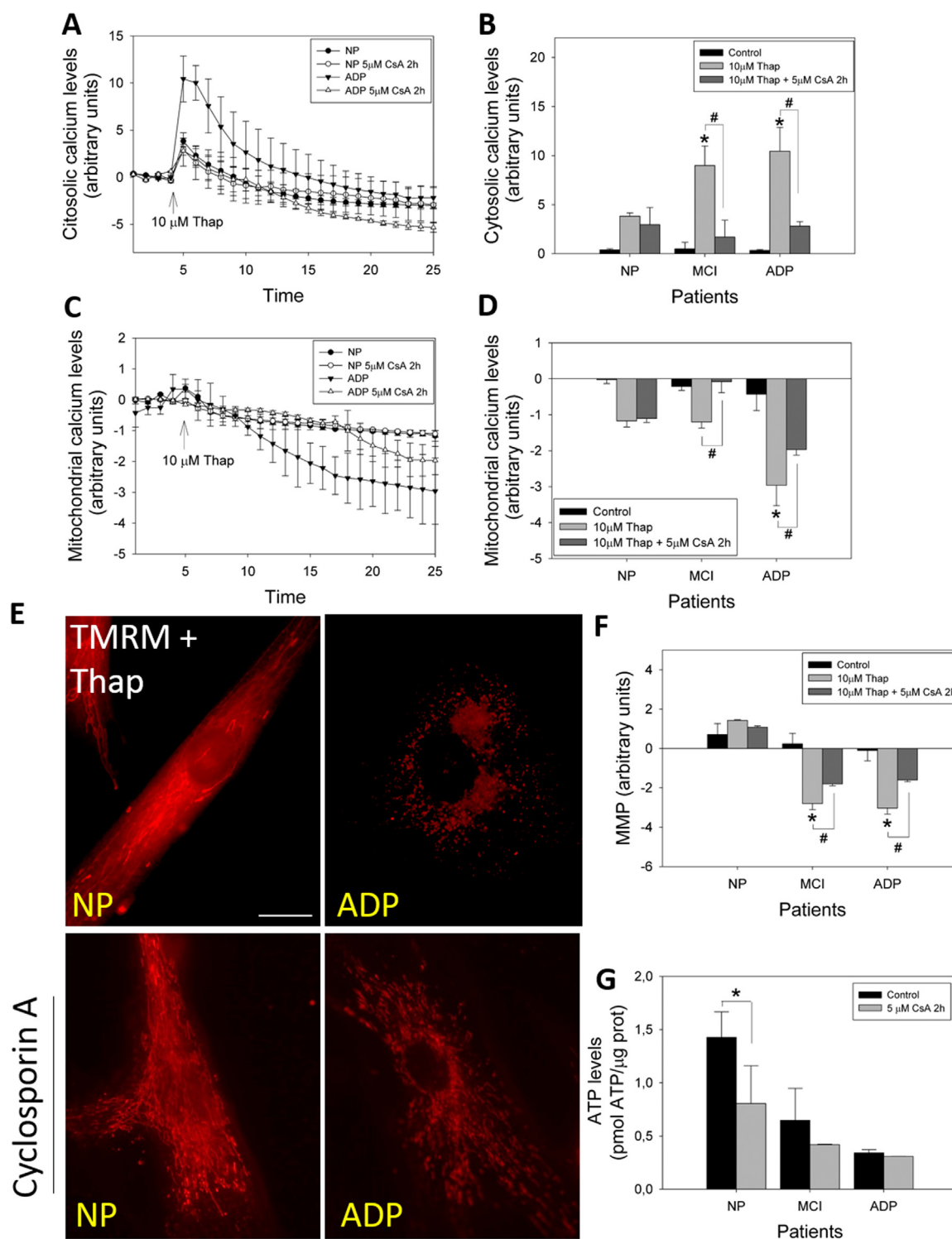
Fig. 5. Cyclosporin A restores calcium regulation in fibroblasts of AD patients. A. Representative trends of cytosolic calcium levels (Fluo-3 signal) over 25 min in severe cognitive impairment AD and control fibroblasts. After 5 min, cells were treated with thapsigargin (arrow). Data are represented as mean ± SE; n = 3 technical replicates for each experiment. **B.** Relative cytosolic calcium levels before and 1 min after treatment with thapsigargin (peak of calcium increase), before and after treatment with CsA. *p < 0.05 indicates differences with control patients, #p < 0.05 indicates differences between control and CsA treatment estimated by Student's *t*-test. **C.** Representative trends of mitochondrial calcium levels (Rhod-2 signal) over 25 min in severe cognitive impairment AD and control fibroblasts. After 5 min, cells were treated with thapsigargin (arrow). Data are represented as mean ± SE; n = 3 technical replicates for each experiment. **D.** Relative mitochondrial calcium levels before and 20 min after treatment with thapsigargin (experiment end point), before and after treatment with CsA. *p < 0.05 indicates differences between AD and control patients, #p < 0.05 indicates differences between control and CsA treatment calculated by Student's *t*-test. **E.** Mitochondrial membrane potential levels (TMRM signal) of fibroblasts treated with thapsigargin, before and after CsA treatment. Bar = 10 μm **F.** Quantification of TMRM signal in basal state, after thapsigargin, and after thapsigargin and 5 μM CsA treatments. *p < 0.05 indicates differences in basal state, #p < 0.05 indicates differences between control and CsA treatment calculated by Student's *t*-test. **G.** Total ATP levels (pmol) normalized by micrograms of protein extracted from control, MCI, and AD fibroblasts before and after CsA treatment. Data are represented as mean ± SE; n = 3 technical replicates for each subject. *p < 0.05 indicates differences with controls calculated by Student's *t*-test.
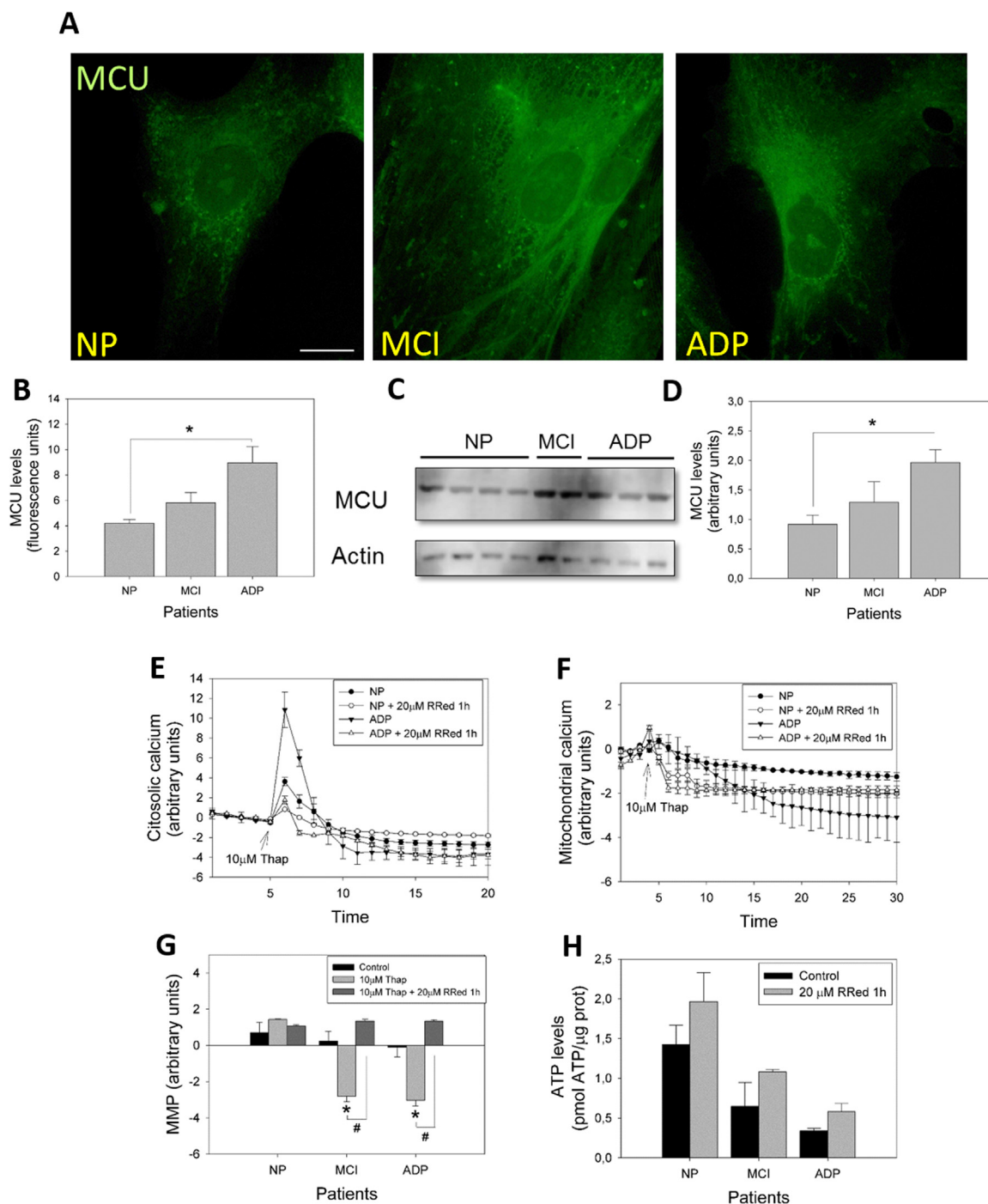
Fig. 6. Inhibition of ER-mitochondrial calcium exchanger prevents mitochondrial bioenergetics dysfunction in AD fibroblasts. A. Representative immunofluorescence images against MCU protein in fibroblasts of control, MCI, and AD patients. Bar = 10 μm **B**. Immunofluorescence quantification of the fluorescence intensity of MCU signal. Data are represented as mean ± SE; n = 3 technical replicates for each subject. *p < 0.05 indicates differences between AD and control patients. **C**. Representative images of protein levels of MCU in AD, MCI, and control patients determined by western blot (see Methods). **D**. Quantitative analysis of relative protein expression. Data are represented as mean ± SE. *p < 0.05 indicates differences between AD and control patients. **E**. Representative trends of cytosolic calcium levels (Fluo-3 signal) over 30 min in AD and control fibroblasts. After 5 min, cells were treated with thapsigargin (arrow). Data are represented as mean ± SE; n = 3 technical replicates for each experiment. **F**. Representative trends of mitochondrial calcium levels (Rhod-2 signal) over 20 min in AD and control fibroblasts. After 5 min, cells were treated with thapsigargin (arrow). Data are represented as mean ± SEM; n = 3 technical replicates for each experiment. **G**. Quantification of TMRM signal in basal state after thapsigargin, and after thapsigargin and RRed treatments. *p < 0.05 indicates differences with basal state, #p < 0.05 indicates differences between control and RRed treatment calculated by Student's *t*-test. **H**. Total ATP levels (pmol) normalized by micrograms of protein extracted from control, MCI, and AD fibroblasts before and after RRed treatment. Data are represented as mean ± SE; n = 3 technical replicates for each subject.

than those in controls cells. Moreover, after a calcium overload stimulus with thapsigargin, mitochondrial calcium levels progressively decrease over time, which supports the hypothesis that AD fibroblast calcium homeostasis is tightly related to mitochondrial injury.

Despite the endoplasmic reticulum (ER) being the main calcium store in a mammalian cell, it has been described that mitochondria are also able to accumulate and regulate calcium homeostasis through direct communication with the ER [8]. Calcium release occurs mainly

through enriched regions of ER-mitochondria associated membranes (MAMs), then calcium enters to the mitochondria through the MCU [8]. Here we observed that MCI and AD patients' fibroblasts show a significant increase in MCU content. Additionally, it has been described that fibroblasts from familial and sporadic AD patients demonstrate an increase in ER-mitochondria contact sites [1]. Together, these results suggest that AD fibroblasts present an increase of ER-mitochondria communication that could be increasing calcium exchange through MCU and oversaturating the mitochondria with calcium. Moreover, despite calcium having a crucial function in regulating mitochondrial metabolism and ATP production [3], excessive calcium in the mitochondria can lead to impairment of function, due to the opening of the mPTP [3]. These effects ultimately could lead to the dissipation of the mitochondrial potential, enhance ROS production, and finally affect ATP production [3,8].

To evaluate the contribution of mitochondrial calcium overload and mPTP opening in mitochondrial dysfunction in AD fibroblasts, we analyzed the principal components of the mPTP [12,15,20,21]. We found that AD fibroblasts showed an increase in gene expression of CypD, ANT, and OSCP, but a decrease in the protein expression of these mPTP proteins. Although different models of upregulation in the mPTP components could lead to an increase in the conformation of the mPTP [28], recent studies have shown that the functional interaction of these proteins have a pivotal role in the mPTP opening [13,2]. In fact, when we analyzed the opening of the mPTP in vivo, we found that in basal conditions, control fibroblasts retain Calcein inside the mitochondria, suggesting that the mPTP is closed. Also, preclinical AD cells showed a partial decrease in the mitochondrial signal of Calcein, suggesting a partially opened state of the mPTP. Interestingly, severe AD cells showed lack of apparent Calcein accumulation in the mitochondria, indicating a permanent opened state of mPTP in these cells.

When we evaluated the effect of mPTP opening in the mitochondrial dysfunction observed in AD fibroblasts, we found that CsA treatment decreased cytosolic ROS, cytosolic calcium levels, and mitochondrial superoxide levels in MCI and severe AD patients. However, inhibition of mPTP with CsA only partially restored mitochondrial calcium and mitochondrial depolarization after thapsigargin treatment. Also, we did not find any changes in ATP levels of MCI, nor severe AD patients' fibroblasts after CsA treatment. In contrast, we observed that the use of the MCU pharmacological blocker RRed [4] completely restored mitochondrial depolarization after thapsigargin treatment, and increased ATP levels in MCI and AD patients after one hour of treatment. These results together suggest that an increase in MCU and MAM contact sites could be leading mitochondria to capture more calcium from the reticulum in AD fibroblasts. This would directly affect mitochondrial calcium content, mitochondrial membrane potential, and later ATP production, since all these events are restored by inhibiting ER-mitochondria communication with RRed. Alternatively, this increase in mitochondria calcium uptake could lead to a permanent opening of the mPTP, which could generate an increase in the cytosolic calcium peak after thapsigargin treatment. These effects could be related to the increase in generation of ROS; when we inhibited mPTP with CsA, these dysfunctional events were prevented.

Previous studies have shown an increase in CypD expression in brain mitochondria from AD patients and AD animal models [11,22]. Contrarily, the use of CsA reduced mitochondrial injury, oxidative stress, and calcium dysregulation in APP transgenic mice and in AD cybrids made with mitochondria obtained from AD patients brain [10,6,9]. This recovery coincides with an improvement in the synaptic function and learning/memory performance in the same AD mouse model and with the reversion of depressed MMP in AD cybrids [10,11,16,6]. Our results indicate that AD fibroblasts show similar signs of mitochondrial injury evident in neurons affected by AD pathology. More importantly, mitochondrial calcium dysregulation with the subsequent mPTP opening seems to be the principal mediator of mitochondrial impairment in AD fibroblasts. The possibility that skin fibroblasts reflect these metabolic changes detected in the AD brain makes this cell type a possible model to establish new targets for early AD diagnostic studies.

Acknowledgements

Disclosure statement

The authors declare that they have no competing interests.

Ethics approval and consent to participate

A total of 11 patients participated in this study after they signed an informed consent form approved by the Bioethics Committee of the Hospital Clínico de la Universidad de Chile. In severe cases of dementia, their caregivers provided the consent. This study has been endorsed by the Bioethics Committee of the Hospital Clínico de la Universidad de Chile and validated by the Universidad Autónoma de Chile.

Appendix A. Supplementary material

Supplementary data associated with this article can be found in the online version at doi:10.1016/j.redox.2018.09.001.

References

[1] E. Area-Gomez, M. Del Carmen Lara Castillo, M.D. Tambini, C. Guardia-Laguarta, A.J. de Groof, M. Madra, J. Ikenouchi, M. Umeda, T.D. Bird, S.L. Sturley, et al., Upregulated function of mitochondria-associated ER membranes in Alzheimer disease, EMBO J. 31 (2012) 4106–4123.

[2] S.J. Beck, L. Guo, A. Phensy, J. Tian, L. Wang, N. Tandon, E. Gauba, L. Lu, J.M. Pascual, S. Kroener, et al., Deregulation of mitochondrial F1FO-ATP synthase via OSCP in Alzheimer's disease, Nat. Commun. 7 (2016) 11483.

[3] P. Bernardi, Mitochondrial transport of cations: channels, exchangers, and permeability transition, Physiol. Rev. 79 (1999) 1127–1155.

[4] K.M. Broekemeier, R.J. Krebsbach, D.R. Pfeiffer, Inhibition of the mitochondrial Ca2+ uniporter by pure and impure ruthenium red, Mol. Cell. Biochem. 139 (1994) 33–40.

[5] F.A. Cabezas-Opazo, K. Vergara-Pulgar, M.J. Perez, C. Jara, C. Osorio-Fuentealba, R.A. Quintanilla, Mitochondrial dysfunction contributes to the pathogenesis of Alzheimer's disease, Oxid. Med. Cell. Longev. 2015 (2015) 509654.

[6] D. Cassarino, R. Swerdlow, J. Parks, D. Parker, J. Bennet, Cyclosporin A increases resting mitochondrial membrane potential in SY5Y cells and reverses the depressed mitochondrial membrane potential of Alzheimer´s disease cybrids, Biochem. Biophys. Res. Commun. 248 (1998) 168–173.

[7] D. Curti, F. Rognoni, L. Gasparini, A. Cattaneo, M. Paolillo, M. Racchi, L. Zani, A. Bianchetti, M. Trabucchi, S. Bergamaschi, S. Govoni, Oxidative metabolism in cultured fibroblasts derived from sporadic Alzheimer´s disease patients, Neurosci. Lett. 236 (1997) 13–16.

[8] O.M. de Brito, L. Scorrano, An intimate liaison: spatial organization of the endoplasmic reticulum-mitochondria relationship, EMBO J. 29 (2010) 2715–2723.

[9] H. Du, L. Guo, F. Fang, D. Chen, A.A. Sosunov, G.M. McKhann, Y. Yan, C. Wang, H. Zhang, J.D. Molkentin, et al., Cyclophilin D deficiency attenuates mitochondrial and neuronal perturbation and ameliorates learning and memory in Alzheimer's disease, Nat. Med. 14 (2008) 1097–1105.

[10] H. Du, L. Guo, W. Zhang, M. Rydzewska, S. Yan, Cyclophilin D deficiency improves mitochondrial function and learning/memory in aging Alzheimer disease mouse model, Neurobiol. Aging 32 (2011) 398–406.

[11] H. Du, S.S. Yan, Mitochondrial permeability transition pore in Alzheimer's disease: cyclophilin D and amyloid beta, Biochim. Et. Biophys. Acta 1802 (2010) 198–204.

[12] J.W. Elrod, J.D. Molkentin, Physiologic functions of cyclophilin D and the mitochondrial permeability transition pore, Circ. J.: Off. J. Jpn. Circ. Soc. 77 (2013) 1111–1122.

[13] E. Gauba, L. Guo, H. Du, Cyclophilin D promotes brain mitochondrial F1FO ATP synthase dysfunction in aging mice, J. Alzheimer'S. Dis.: JAD 55 (2017) 1351–1362.

[14] G.E. Gibson, H. Zhang, L. Toral-Barza, S. Szolosi, B. Tofel-Grehl, Calcium stores in cultured fibroblasts and their changes with Alzheimer's disease, Biochim. Et. Biophys. Acta 1316 (1996) 71–77.

[15] V. Giorgio, E. Bisetto, M.E. Soriano, F. Dabbeni-Sala, E. Basso, V. Petronilli, M.A. Forte, P. Bernardi, G. Lippe, Cyclophilin D modulates mitochondrial F0F1-ATP synthase by interacting with the lateral stalk of the complex, J. Biol. Chem. 284

(2009) 33982–33988.

[16] L. Guo, H. Du, S. Yan, X. Wu, G.M. McKhann, J.X. Chen, S.S. Yan, Cyclophilin D deficiency rescues axonal mitochondrial transport in Alzheimer's neurons, PLoS One 8 (2013) e54914.

[17] D. Hirtz, D.J. Thurman, K. Gwinn-Hardy, M. Mohamed, A.R. Chaudhuri, R. Zalutsky, How common are the "common" neurologic disorders? Neurology 68 (2007) 326–337.

[18] J.R. Hom, R.A. Quintanilla, D.L. Hoffman, K.L. de Mesy Bentley, J.D. Molkentin, S.S. Sheu, G.A. Porter Jr, The permeability transition pore controls cardiac mitochondrial maturation and myocyte differentiation, Dev. Cell 21 (2011) 469–478.

[19] E. Ito, K. Oka, R. Etcheberrigaray, T.J. Nelson, D.L. McPhie, B. Tofel-Grehl, G.E. Gibson, D.L. Alkon, Internal Ca2+ mobilization is altered in fibroblasts from patients with Alzheimer disease, Proc. Natl. Acad. Sci. USA 91 (1994) 534–538.

[20] V. Izzo, J.M. Bravo-San Pedro, V. Sica, G. Kroemer, L. Galluzzi, Mitochondrial permeability transition: new findings and persisting uncertainties, Trends Cell Biol. 26 (2016) 655–667.

[21] E.A. Jonas, G.A. Porter, G. Beutner Jr., N. Mnatsakanyan, K.N. Alavian, Cell death disguised: the mitochondrial permeability transition pore as the c-subunit of the F(1)F(O) ATP synthase, Pharmacol. Res. 99 (2015) 382–392.

[22] M. Manczak, M.J. Calkins, P.H. Reddy, Impaired mitochondrial dynamics and abnormal interaction of amyloid beta with mitochondrial protein Drp1 in neurons from patients with Alzheimer's disease: implications for neuronal damage, Human. Mol. Genet. 20 (2011) 2495–2509.

[23] M.P. Mattson, M. Gleichmann, A. Cheng, Mitochondria in neuroplasticity and neurological disorders, Neuron 60 (2008) 748–766.

[24] G. McKhann, D. Drachman, M. Folstein, R. Katzman, D. Price, E.M. Stadlan, Clinical diagnosis of Alzheimer's disease: report of the NINCDS-ADRDA work group under the auspices of department of health and human services task force on Alzheimer's disease, Neurology 34 (1984) 939–944.

[25] J.C. Morris, The Clinical Dementia Rating (CDR): current version and scoring rules, Neurology 43 (1993) 2412–2414.

[26] J. Naderi, C. Lopez, S. Pandey, Chronically increased oxidative stress in fibroblasts from Alzheimer's disease patients causes early senescence and renders resistance to apoptosis by oxidative stress, Mech. Ageing Dev. 127 (2006) 25–35.

[27] M.J. Perez, D.P. Ponce, C. Osorio-Fuentealba, M.I. Behrens, R.A. Quintanilla, Mitochondrial bioenergetics is altered in fibroblasts from patients with sporadic Alzheimer's disease, Front. Neurosci. 11 (2017) 553.

[28] M.J. Perez, R.A. Quintanilla, Development or disease: duality of the mitochondrial permeability transition pore, Dev. Biol. 426 (2017) 1–7.

[29] M.J. Perez, K. Vergara-Pulgar, C. Jara, F. Cabezas-Opazo, R.A. Quintanilla, Caspase-cleaved tau impairs mitochondrial dynamics in Alzheimer's disease, Mol. Neurobiol. (2017).

[30] H.W. Querfurth, F.M. LaFerla, Alzheimer's disease, N. Engl. J. Med. 362 (2010) 329–344.

[31] R.A. Quintanilla, P.J. Dolan, Y.N. Jin, G.V. Johnson, Truncated tau and Abeta cooperatively impair mitochondria in primary neurons, Neurobiol. Aging 33 (619) (2012) e625–e635.

[32] R.A. Quintanilla, J.A. Godoy, I. Alfaro, D. Cabezas, R. von Bernhardi, M. Bronfman, N.C. Inestrosa, Thiazolidinediones promote axonal growth through the activation of the JNK pathway, PLoS One 8 (2013) e65140.

[33] J.S. Richardson, K.V. Subbarao, L.C. Ang, On the possible role of iron-induced free radical peroxidation in neural degeneration in Alzheimer's disease, Ann. N. Y. Acad. Sci. 648 (1992) 326–327.

[34] J. Sheehan, R. Swerdlow, S. Miller, R. Davis, J. Parks, W.D. Parker, J. Tuttle, Calcium homeostasis and reactive oxygen species production in cells transformed by mitochondria from individuals with sporadic Alzheimer´s disease, J. Neurosci. 17 (12) (1997) 4612–4622.

[35] M. Vangipuram, D. Ting, S. Kim, R. Diaz, B. Schule, Skin punch biopsy explant culture for derivation of primary human fibroblasts, J. Vis. Exp.: JoVE (2013) e3779.

[36] S. Vargas, D. Rangel, F. Quintanilla, R. Rodriguez, Determination of calcium mobility in alkaline-cooked grounded corn in presence of a magnetic field, J. Food Sci. 79 (2014) E1343–E1350.

[37] J. Yao, R.W. Irwin, L. Zhao, J. Nilsen, R.T. Hamilton, R.D. Brinton, Mitochondrial bioenergetic deficit precedes Alzheimer's pathology in female mouse model of Alzheimer's disease, Proc. Natl. Acad. Sci. USA 106 (2009) 14670–14675.